Analyst

PAPER

View Article Online
View Journal | View Issue

Check for updates

Cite this: *Analyst*, 2025, **150**, 4762

# Silica surface modification *via* diazotization of *p*-phenylenediamine: a stationary phase for HPLC

Joseph R. Ezzo, Brandon L. Salazar, Raúl J. Díaz-Santiago and Luis A. Colón *

A phenylenediamine-derived layer was grafted onto superficially porous silica particles through the diazotization of *p*-phenylenediamine (*p*-PDA), circumventing traditional silica silanization reactions. The polyphenylene-type layer was characterized using diffuse reflectance infrared Fourier transform spectroscopy (DRIFTS), X-ray photoelectron spectroscopy (XPS), and elemental analysis. XPS revealed a surface layer containing approximately one nitrogen atom for every three aryl rings. In addition, the layer on silica included azo-linkages of aryl groups and amine functionalities, with one amine group per four to five benzene rings. Elemental analysis indicated that surface coverage of the aryl groups could be modulated by adjusting the reaction conditions, thereby enabling control over surface loading while reducing potential pore obstruction. A *p*-PDA-derived layer having 2–4 rings per $nm^2$ proved effective as a stationary phase for high-performance liquid chromatography (HPLC) and exhibited excellent hydrolytic stability under relatively harsh acidic conditions (0.5% TFA at 80 °C). Furthermore, beyond small molecules, the new phase showed promise for peptide separation.

Received 13th August 2025,
Accepted 25th September 2025

DOI: 10.1039/d5an00869g

rsc.li/analyst

Open Access Article. Published on 25 2025. Downloaded on 05.01.2026 23:39:58.
This article is licensed under a Creative Commons Attribution 3.0 Unported Licence.

## Introduction

Silica is one of the most widely used support materials in many fields. In chromatographic applications, silica is used extensively as a support material to hold the stationary phase, which is responsible for the separation of chemical compounds in a mixture. Silica is typically used because of its high mechanical stability, high surface area, and simple surface chemistries.[1] Chromatographic stationary phases with a specific functionality are produced by selecting the appropriate reactant to chemically modify the silica surface; most typically, this approach is based on the silanization of the silanol groups on the silica surface.[1–3] Organosiloxane linkages (surface-O–Si–C) are formed between the silica surface and desired organic species, producing a monomeric layer at the surface of the silica support. Multilayers of organosilanes (*i.e.*, polymeric layers) were attached using similar procedures. This is a commonly used approach for the preparation of most commercially available chromatographic materials (*i.e.*, bonded phases). Although a variety of chemically bonded phases exist, the most common ones usually consist of hydrocarbon chains ($C_{18}$ and $C_8$ are the most popular) and are typically used in chromatographic reversed-phase separation mode.

The vast majority of silica modifications to produce stationary phases for chromatography rely on chemical attachment *via* silanization chemistry. Herein, we report an alternative method for forming a surface-confined layer on silica supports for use in chromatography, without silanization reactions. This method uses a highly reactive diazonium species. Chemical functionalization of metallic surfaces by means of diazonium salts has become commonplace,[4] but not for silica. Diazonium chemistry is highly attractive because of the relative simplicity of the reaction and high reactivity of the diazonium species formed. It provides a versatile method to modify conducting and non-conducting substrates, which is convenient and efficient.[5–8] Most typically, the reaction proceeds *via* the formation of diazonium salts from an aryl amine in the presence of a reducing agent (*e.g.*, sodium nitrite) and an acid catalyst. The aryl diazonium species is then reduced resulting in the grafting of phenyl moieties on the surface.[9–11] The *in situ* diazotization approach has been used for surface modification of various carbon materials,[9,10,12–14] as well as metals and metal oxides.[5–8,15–19]

A few reports have demonstrated the use of diazonium chemistry to specifically modify carbon materials;[20–23] these were then explored for chromatographic applications. However, the direct modification of silica *via* diazonium chemistry to produce chromatographic materials, particularly for high performance liquid chromatography (HPLC), has not been reported. Silica modification *via* diazonium chemistry appears to have been limited to the fabrication of nanocomposites,[24–27] and the preparation of filler particles for polymeric matrixes.[28]

*Department of Chemistry, Natural Sciences Complex, University at Buffalo, State University of New York, Buffalo, New York 14260-3000, USA.*
*E-mail: lacolon@buffalo.edu*



This journal is © The Royal Society of Chemistry 2025

Open Access Article. Published on 25 2025. Downloaded on 05.01.2026 23:39:58.
This article is licensed under a Creative Commons Attribution 3.0 Unported Licence.

In the present study, our objective was to explore the versatility of diazonium chemistry for modifying silica particles for chromatographic applications without silanization reactions. We demonstrated that the silica-based stationary phase prepared using this approach is hydrolytically stable under acidic conditions in liquid chromatography. Diazotization of *p*-phenylenediamine was used to covalently graft phenylene groups, also containing amino moieties, to the surface of core–shell (or superficially porous) silica microspheres. We selected these particles because of their improved efficiencies and faster separations.[29–31] Reacting an excess of *p*-phenylenediamine allowed the formation of a surface-confined polymeric-like layer with multiple attachments to the silica support.

# Experimental

## Materials

ACS grade sodium nitrite was obtained from Avantor Performance Chemicals. HPLC-grade methanol, acetonitrile, ACS-grade potassium bromide, and concentrated hydrochloric acid were obtained from Fisher Scientific (Fair Lawn, NJ, USA). The *p*-phenylenediamine used in the diazotization reactions, toluene, ethylbenzene, propylbenzene, butylbenzene, and amylbenzene were purchased from Sigma-Aldrich (St Louis, MO, USA). Trifluoroacetic acid (TFA) was obtained from EDM Millipore (Danvers, MA, USA). Kinetex® core shell silica particles (5 μm particle diameter, 100 Å pore diameter, surface area 107 $m^2\ g^{-1}$) were obtained from Phenomenex (Torrance, CA, USA), and Halo® silica particles (2 μm particle size, 90 Å pore size, surface area 131 $m^2\ g^{-1}$) were obtained from Advanced Materials Technologies (Wilmington, DE, USA). Toluene and anhydrous decane were purchased from Sigma-Aldrich (St Louis, MO, USA), while *p*-aminophenyltrimethoxysilane (*p*-APTMS) from Gelest, Inc. (Morrisville, PA, USA). All water used was deionized and filtered (0.2 μm) in-house with a Barnstead International EASYPure II water purification system. Nitrogen gas (99.995% purity) was obtained from Praxair (Danbury, CT, USA). The 10-peptide standard sample mix (PepMix) was obtained from Agilent Technologies (Santa Clara, CA, USA).

## Silica modification with *p*-phenylenediamine

Surface modification of the superficially porous silica particles was performed under acidic conditions. Low-temperature modifications were performed in an ice bath or a recirculating refrigerated bath to stabilize the diazonium intermediates and limit the reaction kinetics. *The diazonium intermediates were created in situ adding the corresponding reagents dropwise, which avoided any vigorous reaction due to the evolution of gases (mostly nitrogen), even at room temperature.* The reaction conditions were adjusted in terms of the reaction time and the quantity of *p*-PDA added to produce a material suitable for effective chromatographic applications. In one example reaction using Kinetex® core–shell silica particles, 100 mg of the silica particles were suspended in 15 mL of a 1.5 M hydrochloric acid solution under magnetic stirring at 200 RPM. Subsequently, an amount of *p*-PDA was added to the reaction vessel and given adequate time to dissolve (*e.g.*, 139 mg for a 15 : 1 molar ratio of diamine to surface silanol, assuming a fully hydroxylated surface of 8 μmol OH per $m^2$). Finally, sodium nitrite was added dropwise to the mixture to initiate the reduction of the amine (*e.g.*, 3 mL of 1.0 M $NaNO_2$ for the reaction containing 139 mg of *p*-PDA). The reaction was allowed to proceed for a specified time under continuous magnetic stirring. The products were isolated and washed with acetonitrile (AcN), methylene chloride (dichloromethane) and/or tetrahydrofuran (THF), water ($H_2O$), and acetone. Finally, the products were dried overnight at 100 °C under a vacuum. The reactions were scaled up by increasing the reagent quantities proportionally by a factor of three to produce adequate quantities of material to pack the chromatographic columns. The conditions were adjusted slightly for the Halo® particles, accounting for the difference in surface area. For example, 350 mg of the 2 μm Halo® particles were added to 56 mL of a 1.5 M hydrochloric solution in a double-jacketed round bottom flask while stirring at 200 RPM. The flask was connected to a recirculating bath to maintain the reaction temperature for the entirety of the reaction. Next, *p*-PDA was added such that the molar ratio to the isolated silanol groups was 15 : 1. After allowing approximately 5 minutes for the contents in the flask to stir in solution, 11 mL of 1.0 M sodium nitrite solution were added dropwise to the flask in 10 minutes using a syringe pump (Harvard Apparatus, PHD 2000 Infusion, Holliston, MA, USA). The reaction was left to proceed uninterrupted for a given time. Afterwards, the particles were washed with AcN, THF, water, and acetone, in that order. The functionalized particles were dried overnight in a vacuum oven at 120 °C.

For comparison purposes in the hydrolytic stability test, silica particles were also modified *via* silanization with *p*-aminophenyltrimethoxysilane (*p*-APTMS) using a procedure previously published from our group.[32] Briefly, Kinetex® core shell silica particles were boiled in water for 1 h to maximize the number of –OH groups at the surface. The hydrolyzed particles were decanted and dried at 120 °C. In a round bottom flask containing anhydrous deacane, the silica particles were added in a proportion of 100 mg per 2.5 mL of decane. Water was added to the flask in a 1 : 10.5 (silanol : $H_2O$) molar ratio and the solution was stirred for 1 h. Then, *p*-APTMS was added in a 1 : 1.05 (silanol : *p*-APTMS) molar ratio. The reaction mixture was then stirred for 24 h at 130 °C while keeping the system under nitrogen. The collected particles were rinsed three times with toluene, methanol, methanol/water (50 : 50 v/v) and acetone and recovery *via* centrifugation after each rinse.

## Material characterization

The surface composition of the modified silica particles was analyzed by diffuse reflectance infrared Fourier transform spectroscopy (DRIFTS) using a PerkinElmer Spectrum Two FT-IR spectrometer (Waltham, MA) equipped with a DRIFTS

Open Access Article. Published on 25 2025. Downloaded on 05.01.2026 23:39:58.
This article is licensed under a Creative Commons Attribution 3.0 Unported Licence.

optical stage. Prior to the analysis, the modified silica samples were dried overnight at 120 °C under vacuum and stored in a desiccator to limit water adsorption on the surface. The samples were diluted in a KBr matrix (1 : 10 mass ratio) and ground using a mortar and pestle prior to the analysis. A 20 mg sample cup was used for each analysis. Pure potassium bromide was used as the background. A portion of the unmodified core–shell silica particles was used as a blank. Spectra were obtained by accumulating 300 total scans from 4000 $cm^{-1}$ to 400 $cm^{-1}$ with a resolution of 2 $cm^{-1}$. Surface coverage was estimated by elemental analysis. Carbon, hydrogen, and nitrogen elemental analyses were performed by Atlantic Microlabs Inc. (Norcross, GA, USA) or in-house using a Thermo Scientific Elemental Analyzer (model FLASH EA 1112, Milano, Italy). The surface area and pore dimensions were estimated by gas adsorption analysis using a Quantachrome Nova 1200e surface area and pore analyzer (Boynton Beach, FL), which makes use of the Brunauer–Emmett–Teller (BET) method for surface area and the Barrett–Joyner–Halenda (BJH) method for pore size and volume analysis.[33,34] Nitrogen gas was used as the adsorbate in all cases. The samples were degassed overnight at 120 °C prior to analysis. The surface area of unmodified silica was determined to estimate the amount of each reagent in relation to the silica surface hydroxyl groups (fully hydroxylated silica surface with 8 μmol $m^{-2}$ of reactive silanol groups).

The percentage of carbon determined by elemental analysis was used to calculate the surface coverage of the silica material. Because the carbon content originates exclusively from the aromatic rings, the number of rings per unit area was calculated according to the following equation:

$$\text{rings per nm}^2 = \frac{(\%C_s)}{(100 - \%C_s - \%N - \%H) \times 6M_c \times S_{bet}} \times \frac{N_A}{1 \times 10^{18}}$$

where $\%C_s$, $\%N_s$, and $\%H_s$ are the percentages of carbon, nitrogen, and hydrogen, respectively, in the sample obtained by elemental analysis. $M_c$ is the molar mas of carbon, $S_{bet}$ the surface area in g $m^{-2}$ of the unmodified silica particles based on nitrogen adsorption analysis, and $N_A$ is Avogadro's number.

X-ray photoelectron spectroscopy (XPS) was performed using a Physical Electronics PHI Versaprobe 5000 instrument (Chanhassen, MN, USA) equipped with a hemispherical energy analyzer. A monochromic Al-Kα X-ray source (1486.6 eV) was operated at 25.3 W and 15 kV. The analyzer operated at a pass energy of 117.5 eV for survey acquisitions and 23.5 eV for high-resolution acquisitions. The X-ray spot size was set to 100 μm for high-sensitivity acquisition. The energy resolution was 1.0 eV for the survey spectra and 0.1 eV for high-resolution spectra. The operating pressure of the analysis chamber was $<4.0 \times 10^{-6}$ Pa ($3.0 \times 10^{-8}$ Torr), and the background pressure was $<1.0 \times 10^{-6}$ Pa ($7.5 \times 10^{-9}$ Torr). Dual-charge neutralization was utilized to reduce the effects of charging on the acquired signal. The binding energies were calibrated by setting the CH peak in the $C_{1s}$ envelope to 284.8 eV.

### Column packing and chromatographic testing

The chromatographic columns were packed by means of the slurry-packing method using a 4% slurry concentration. For example, 200 mg of the packing material was sonicated in methanol or 75 : 25 MeOH : THF for 20 min. The slurry solution was transferred to a 5 mL column-packing reservoir attached to a 2.1 mm i.d. × 50 mm long column equipped with a 0.5 μm frit at the outlet end. Column hardware and frits were purchased from Idex (Lake Forest, IL, USA) and Shepard Industries (Port Matilda, PA, USA), respectively. The chromatographic column packing was completed at a pressure of approximately 10 000 psi and maintained for 15 min. The pump was turned off, and the columns were allowed to depressurize before assembly of the entrance frit and end fittings. The column was then flushed with pure MeOH and the mobile phase for at least 10 min before testing.

HPLC experiments were performed using an Agilent 1100 system (Palo Alto, CA, USA) equipped with a diode array detector or a Waters I Class UPLC unit (Milford, MA, USA) equipped with a UV detector. For the Agilent HPLC unit, system control and data collection were performed using ChemStation for LC 3D (Rev. A.09.03) software from Agilent Technologies. The Waters system was controlled using Empower software from Waters. When using gradient elution, the sloping baseline in chromatograms was subtracted using OriginPro 2025b software (OriginLab Corp., Northampton, MA, USA); all final plots were also displayed using OriginPro 2025b. HPLC experiments were typically carried out at room temperature using acetonitrile–water mixtures as mobile phases, unless otherwise specified. Prior to use, all samples and mobile phases were filtered through 0.2 μm nylon filters.

For the stability test, the mobile phase consisted of 0.5% TFA in a 50/50 mixture of water and acetonitrile. The mixture was sonicated for 20 min to remove dissolved gas. The columns were maintained at 80 °C using the TFA acidified mobile phase. Once columns reached temperature, the mobile phase was run through the column for a total of twenty hours at 0.2 mL $min^{-1}$, equivalent to 2400 column volumes, making injection of a probe compound every 30 min. The column was then rinsed with water for 30 min to remove the acid and equilibrated with a 50/50 mixture of water and acetonitrile. A sample of toluene, ethylbenzene, and propylbenzene (100 μg $mL^{-1}$) in a 50/50 mixture of water and acetonitrile was used to compare the retentivity of the column before and after the acid degradation test.

## Results and discussion

### Silica modification *via p*-phenylenediamine diazotization

The use of diazonium salts to modify the surface chemistry across various materials has been both prominent and relevant in multiple fields.[5–8,35] Although it has been established that these salts react with oxides, the direct application of diazonium chemistry to modify the surface of silica materials has been notably limited and appears to be non-existent in chro-

 This journal is © The Royal Society of Chemistry 2025

Open Access Article. Published on 25 2025. Downloaded on 05.01.2026 23:39:58.
This article is licensed under a Creative Commons Attribution 3.0 Unported Licence.

matographic applications. The versatility and simplicity of silica modification *via* diazonium chemistry are particularly appealing. Therefore, we investigated the surface modification of superficially porous silica particles *via* diazonium chemistry by the *in situ* diazotization of *p*-PDA using sodium nitrite in combination with hydrochloric acid to produce nitrous acid. The nitrous acid converts the aryl amines present on the *p*-PDA to aryl diazonium cations. The diazonium species reacted with the electron-rich silica surface,[36] forming a polyphenylene-like layer on the surface of the silica particles. An idealized schematic representation of the surface modification is shown in Fig. 1.

### Material characterization

The successful grafting of *p*-PDA onto superficially porous silica particles was confirmed by diffuse reflectance infrared Fourier transform spectroscopy (DRIFTS). Fig. 2 shows the DRIFTS spectra of the modified (red trace) and unmodified (black trace) silica particles. The unmodified silica shows characteristic peaks corresponding to the isolated silanol stretching vibration (3756 $cm^{-1}$), stretching modes of hydrogen bound water (3315 $cm^{-1}$), deformation vibrations of adsorbed water (1630 $cm^{-1}$), asymmetric stretching modes of the siloxane backbone (1175 $cm^{-1}$), and symmetric stretching of siloxane bonds (805 $cm^{-1}$).[37–39] The silica overtones at 1988 $cm^{-1}$ and 1870 $cm^{-1}$ are also clearly displayed.[40–42] The spectrum of the modified material, on the other hand, exhibits new IR signatures indicative of the C–H stretch of $sp^2$ hybridized carbon atoms (3060–2925 $cm^{-1}$), the $NH_2$ deformation of amines (1650 $cm^{-1}$), IR signals of the aromatic ring stretches (1597 $cm^{-1}$ and 1495 $cm^{-1}$), and the vibration corresponding to C–H out of plane deformation characteristic of benzene rings (700 $cm^{-1}$).[37,38] It would be reasonable to expect bands characteristic of stretching modes of amines in the 3350–3450 $cm^{-1}$ region; however, these were not apparent most likely because such can be masked by the band corresponding to OH. A very small shoulder peak at 1430 $cm^{-1}$ can be attributed to azo bonds,[37] which are present in the polymeric-like layer connecting phenyl groups.

Modification of the silica particles results in a decrease in the relative intensity of the band associated with the free silanol stretching band (3756 $cm^{-1}$), suggesting that the *p*-PDA

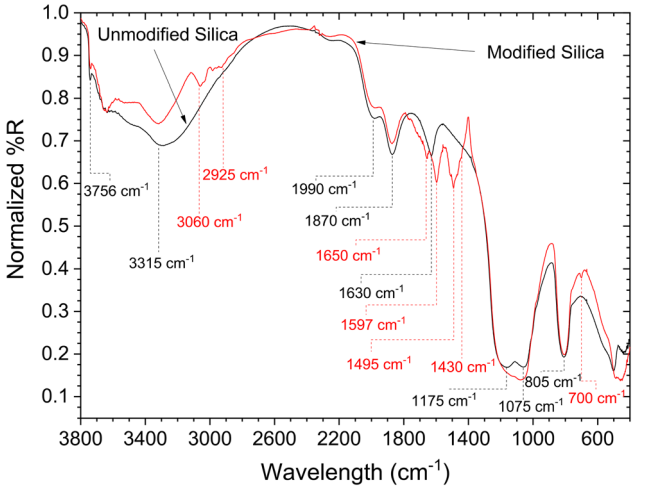


**Fig. 2** DRIFTS spectra of superficially porous silica particles (Kinetex® core–shell particles) before (black trace) and after (red trace) modification with *p*-PDA *via* diazotization (4 rings per $nm^2$).

layer formed is bound to the surface by reacting with the surface silanol groups. This is substantiated by the lack of a peak corresponding to a silicon–carbon bond. Our observations agree with those reported for the functionalization reaction of aminophenyl groups with silica–carbon nanocomposites used as anode materials in lithium-ion batteries.[24] The attachment of *p*-PDA to silica *via* silanol groups should yield a silicon atom bonded to an aromatic ring through a silyl ether linkage;[11,43] this should result in a characteristic IR band at approximately 1240 $cm^{-1}$. However, this band was obstructed by the IR absorption of the siloxane bond, indicating the need for other spectroscopic techniques to elucidate the mechanism of surface binding.

X-ray photoelectron spectroscopy (XPS) was used to examine the surface chemistry of the modified silica particles. An XPS survey spectrum of the modified SPPs particles (~4 rings per $nm^2$) revealed the presence of five peaks corresponding to $C_{1s}$, $N_{1s}$, $O_{1s}$, $Si_{2p}$, and $Cl_{2p}$ (Fig. S1 in the SI). The atomic surface percentages are listed in Table 1. The presence of the $Cl_{2p}$ peak in the XPS spectrum indicates that chlorine anions interact electrostatically with protonated amine groups associated with nitrogen at the surface (see below). Chlorine is

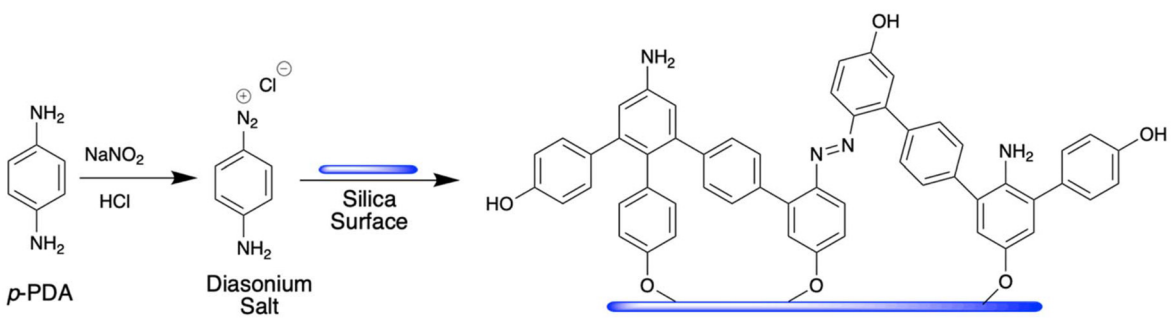


**Fig. 1** An idealized schematic representation of the polyphenylene-like layer on the silica surface.

Open Access Article. Published on 25 2025. Downloaded on 05.01.2026 23:39:58.
This article is licensed under a Creative Commons Attribution 3.0 Unported Licence.

**Table 1** Atomic percentages determined by XPS of the *p*-PDA-derived layer on silica

| Element | C | N | O | Si | Cl |
|---|---|---|---|---|---|
| Surface atomic composition (%) | 36 | 2 | 30 | 23 | 1 |

present in the chemical reaction because HCl is the acid used during diazotization. High-resolution XPS and deconvolution of the $Cl_{2p}$ spectrum (Fig. S2 in SI) reveals two pairs of spin–orbit split contributions. The lower-energy pair is attributed to the chlorine anions associated with the protonated amine groups. The ionic interactions between these two species were responsible for more than 80% of the chlorine present. Two additional peaks in the $Cl_{2p}$ spectrum at 203.1 eV and 204.2 eV correspond to a carbon–chlorine bond. This is likely the result of benzenediazonium chloride decomposing to chlorobenzene in a process similar to that observed for other halides.[44] In general, however, the amount of chlorine is very small.

Fig. 3 illustrates the high-resolution XPS spectra of carbon and nitrogen for the phenylenediamine-derived layer on silica. The $C_{1s}$ core electron spectrum (Fig. 3A) shows signal contributions from different binding energies, the most pronounced of which corresponds to the carbon–carbon and carbon–hydrogen bonding present in the synthesized layer on the silica surface. Additionally, the broad peak centered at 291.6 eV is a satellite peak corresponding to the π–π* transition in aromatic compounds and originating from ring excitation by ejected photoelectrons.[45] The peak in Fig. 3A at 286.1 eV is indicative of a carbon–oxygen bond,[46] which is characteristic for carbon atoms that are bonded simultaneously to both silicon and oxygen atoms.[47] This peak, in conjunction with the lack of the typical signals corresponding to silicon carbon bond in the $Si_{2p}$ spectrum around 100–101 eV,[48,49] (see Fig. S3 in SI) and around 282–283 eV in the carbon spectrum, suggests that covalent attachment of the phenylene-like polymeric layer to the silica support occurs through the oxygen atoms. Further, silicon atoms with a mixed environment of oxygen and carbon bonds display a spectrum with binding energy at 103 eV;[47–49] this is clearly displayed in Fig. S3 in SI. The prevalence of the carbon–oxygen bond signature also indicates that it is likely that aryldiazonium cations are also converted to phenols during the synthetic process. A small DRIFTS signal at 3650 $cm^{-1}$ is also indicative of free or unbonded hydroxyl group often found in phenols.[50]

The XPS peak present at 287.8 eV is attributed to carbon nitrogen bonds of the remaining amines and azo groups present in the material at the silica surface. One would expect two distinct forms of nitrogen on the phenylenediamine-derived layer on the silica particles, namely amines and azo groups. Analysis of the $N_{1s}$ spectrum (Fig. 3B), however, reveals three peaks. The peaks at 399.7 eV and 402.1 eV are indicative of the C–N bonds of the amines and quaternary amine groups respectively.[51–53] The remaining peak at 400.7 eV is attributed to azo groups.[46,51,54] Analysis of the peak areas suggests that approximately 40% of the nitrogen atoms exist as azo bridges. Assessment of the atomic surface percentages of carbon (36%) and nitrogen (2%) revealed the presence of one nitrogen atom every three aromatic rings. The result agrees with the observations from elemental analysis (*i.e.*, 14.5% C and 0.87% N by mass: 1 N per 2.7 benzyl rings). This is indicative of approximately one amine group per 4–5 benzene rings.

The diazotization reaction proceeded in acidic medium in the presence of nitrite as the reducing agent to form the

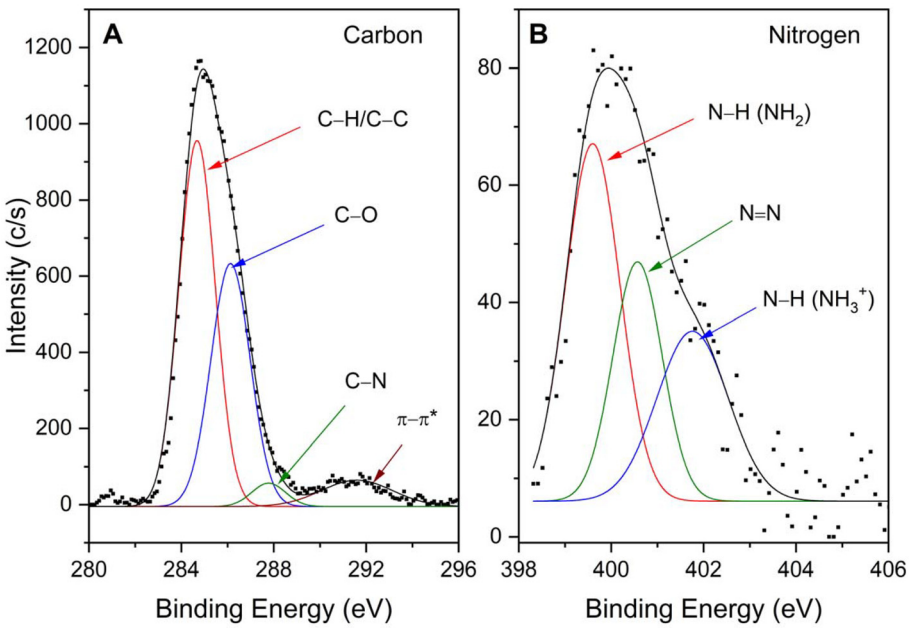


**Fig. 3** High-resolution XPS spectra and deconvoluted peaks corresponding to (A) $C_{1s}$ and (B) $N_{1s}$ of the *p*-PDA-derived layer on the silica particles.


This journal is © The Royal Society of Chemistry 2025

Open Access Article. Published on 25 2025. Downloaded on 05.01.2026 23:39:58.
This article is licensed under a Creative Commons Attribution 3.0 Unported Licence.

*p*-PDA-derived layer on the silica particles. We determined the surface coverage (benzyl rings per $nm^2$ and/or μmol rings per $m^2$) of the *p*-PDA-derived layer on the silica particles as a function of the molar ratio of *p*-PDA to surface silanol, assuming a fully hydroxylated silica surface of 8 μmol $m^{-2}$, as well as the reaction time. These experiments were conducted on the 5 μm-Kinetex® core–shell silica particles (100 mg of silica suspended in 15 mL of 1.5 M hydrochloric) under magnetic stirring in an ice bath to maintain the temperature below 5 °C. The concentrations of hydrochloric acid (1.5 M) and sodium nitrite (1.0 M) solutions added to the diazotization reaction were kept constant, but the amount of sodium nitrite added was adjusted to maintain a constant ratio of nitrite to *p*-PDA in the reactions (*i.e.*, one nitrite per amine). The reaction time was studied by maintaining the *p*-PDA : SiOH ratio at 15 : 1. The elemental composition and surface coverage as a function of *p*-PDA in the reaction and the reaction time are included in Tables 2 and 3, respectively.

The results indicate that decreasing both the reaction time and the molar ratio of *p*-PDA to silanol decreased the extent of surface modification, with the effects being more pronounced in the latter. Although not well appreciated in the DRIFTS spectra, there was also a decrease in the intensity of both the ring stretching and amine bending vibrations signals. Additionally, the intensity of the free silanol stretching vibration (3756 $cm^{-1}$) showed an inverse relationship with these DRIFTS bands, providing further evidence of decreased surface loading at low *p*-PDA-to-silanol ratios.

Typically, diazotization reactions are performed below 5 °C to prolong the lifetime of the highly reactive diazonium ion. However, we also modified silica particles *via* the diazotization of *p*-PDA at room temperature (23 °C). The reactions were performed using Halo® silica particles (2 μm diameter). The reaction at room temperature proceeded much faster than that at low temperature, visibly noticeable by the fast formation of a foam-like layer with the evolution of bubbles, presumably due to the fast formation of nitrogen gas. The addition of the nitrite solution to the reaction mixture was then performed for a period of 10 min (using a syringe pump), instead of the 3 min manual drop addition used for the reactions at low temperature (~3 °C). Table S1 in the SI shows the elemental analysis of the reactions at room temperature (23 °C) and 3 °C with the corresponding surface coverage. After 2 h of adding the nitrite solution at room temperature, the reaction yielded particles containing approximately 2 rings per $nm^2$ (3.1 μmol $m^{-2}$). Adding nitrite at the same rate at 3 °C also provided particles with 2 rings per $nm^2$, but the reaction required 24 h.

The XPS studies shown above revealed the presence of residual amines on the surface. The residual amine content (*i.e.*, unreacted amines after the diazotization of *p*-PDA) was examined by reacting the *p*-PDA-modified particles with benzoyl chloride to form the corresponding amide.[55] The carbon content was measured by elemental analysis before and after the reaction. The increase in the percentage of carbon corresponding to the benzoyl moiety that reacted with the free amine. The results of the elemental analyses (see Tables S2 and S3 in the SI) indicated that there was one residual amine every 3–4 rings for both *p*-PDA particles prepared at room temperature and at 3 °C.

**Table 2** Elemental composition and surface coverage for different *p*-PDA-derived layers on silica particles as a function of the *p*-PDA : SiOH ratio in the reaction[a]

| *p*-PDA : SiOH ratio | %C | %N | %H | Surface coverage (rings per $nm^2$) |
|---|---|---|---|---|
| 5 : 1 | 0.34 | 0.16 | 0.17 | 0.3 |
| 10 : 1 | 1.60 | 0.33 | 0.22 | 1.9 |
| 15 : 1 | 14.4 | 0.87 | 0.73 | 13 |

[a] The reaction of *p*-PDA on the 5 μm-Kinetex® core–shell silica particles proceeded for 12 h.

**Table 3** Elemental composition and surface coverage for different *p*-PDA-derived layers on silica particles as a function of the reaction time[a]

| Reaction time (h) | %C | %N | %H | Surface coverage (rings per $nm^2$) |
|---|---|---|---|---|
| 3 | 2.6 | 0.16 | 0.27 | 2.1 |
| 6 | 5.0 | 0.33 | 0.41 | 3.8 |
| 9 | 5.9 | 0.41 | 0.52 | 4.9 |
| 12 | 14.4 | 0.87 | 0.73 | 13 |

[a] A *p*-PDA : SiOH ratio of 15 : 1 was used in all reactions.

## Chromatographic testing

Computational modeling has indicated that by means of silanization, the maximum number of aminophenyl rings that can be attached to the silica surface for a complete monolayer is approximately 3–4 rings per square nanometer.[32] The data presented in Tables 2 and 3 suggest that quantities exceeding this threshold can be achieved depending on the reaction conditions. A high surface coverage (>4 rings per $nm^2$) indicates vertical polymerization of phenyl rings, which can be detrimental to chromatographic applications. An excessive amount of phenyl groups may also clog the pores of the silica particles and/or introduce too much material as the stationary phase, negatively affecting the mass transfer kinetics and reducing the chromatographic performance. The chromatographic testing was performed on columns prepared from materials listed in Table 3. From here on, we refer to the number of rings per $nm^2$ by rounding the values in Table 3 to the nearest whole number (*i.e.*, 2.1 to 2 rings per $nm^2$ and 3.8 to 4 rings per $nm^2$). Fig. 4 illustrates the impact of an HPLC column packed with 5 μm Kinetex® core–shell silica particles containing a *p*-PDA-derived layer of 13 rings per $nm^2$ compared to a column containing particles with 4 rings per $nm^2$. The chromatograms clearly show that large surface coverage is unfavorable for the separation of the probe compounds.

We obtained favorable chromatographic performance with columns packed with particles containing 2–4 rings per $nm^2$, particularly with 2 μm particulates (*i.e.*, Halo® core–shell silica

Open Access Article. Published on 25 2025. Downloaded on 05.01.2026 23:39:58.
This article is licensed under a Creative Commons Attribution 3.0 Unported Licence.

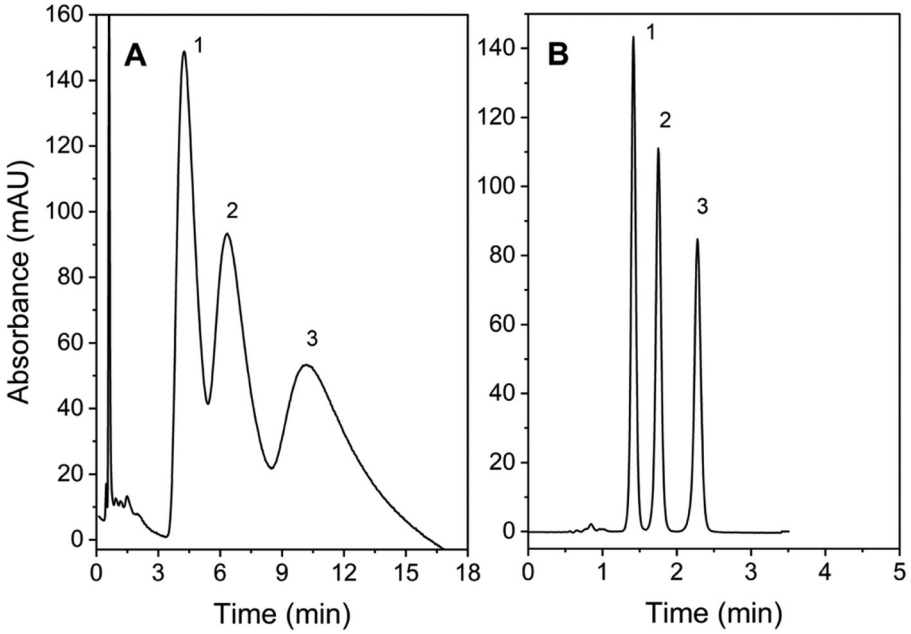


**Fig. 4** Chromatograms illustrating the separation of model compounds in columns with *p*-PDA-derived phases containing (A) 13 rings per nm$^2$ and (B) 4 rings per nm$^2$ on 5 μm-Kinetex® core–shell silica particles (columns dimensions: 50 mm length, 2.1 mm i.d.). A mobile phase of 50/50 acetonitrile/water was used at a flow rate of 0.2 mL min$^{-1}$; UV detection was performed at 210 nm. Compounds: (1) toluene, (2) ethylbenzene, and (3) propylbenzene (100 μg mL$^{-1}$ each, 1 μL injection).

particles). The separation of the model compounds in columns packed with *p*-PDA-derived phases containing 2 and 4 rings per nm$^2$ is shown in Fig. 5. As expected, using 2 μm particles improved separation efficiency. Under identical separation conditions, the column with the 4 rings per nm$^2$ *p*-PDA-derived phase (Fig. 5B) showed a slightly higher retention than

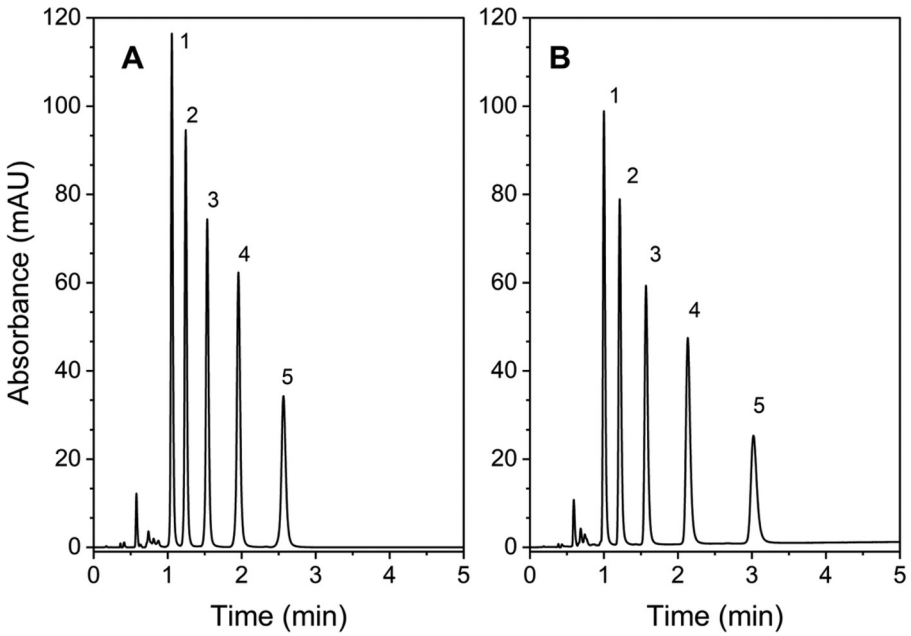


**Fig. 5** Chromatograms illustrating the separation of model compounds in columns with *p*-PDA-derived phases containing (A) 2 rings per nm$^2$ and (B) 4 rings per nm$^2$ on Halo® core–shell silica particles (columns dimensions: 50 mm length, 2.1 mm i.d.). A mobile phase of 45/55 acetonitrile/water was used at a flow rate of 0.2 mL min$^{-1}$; UV detection was performed at 210 nm. Compounds: (1) toluene, (2) ethylbenzene, (3) propylbenzene, (4) butylbenzene, and (5) amylbenzene (100 μg mL$^{-1}$ each, 1 μL injection).

 This journal is © The Royal Society of Chemistry 2025

Open Access Article. Published on 25 2025. Downloaded on 05.01.2026 23:39:58.
This article is licensed under a Creative Commons Attribution 3.0 Unported Licence.

the one containing 2 rings per nm$^2$, noticing that an increase in retention is expected with an increase in the amount of the stationary phase. Table S4 in the SI provides chromatographic metrics (*e.g.*, theoretical plates, retention factor, and asymmetry factors) for chromatograms shown in Fig. 5. Batch-to-batch retentivity (*i.e.*, retention factor) and surface coverage data is also provided as SI (Tables S5 and S6).

The separation of many compounds is facilitated by using acidic mobile phases;[56–58] this has also become a common place when interfacing HPLC and mass spectrometry (MS),[59–65] and long-lasting stationary phases are preferred. Using a conventional accelerated stability test,[66–68] columns packed with *p*-PDA-derived materials were shown to be stable under low-pH mobile phase conditions. This is illustrated in Fig. 6, in which the retention of propylbenzene was plotted as a function of the exposure time of the column to acidic conditions at elevated temperatures. A column containing the material prepared by conventional silanization was also included for comparison (*i.e.*, aminophenyltrimethoxysilane). The percent retention loss was minimal when using the columns containing silica particles with the *p*-PDA-derived layers (2 and 4 rings per nm$^2$), whereas the *p*-APTMS-derived phase degraded very quickly during the test, as indicated by the relatively fast loss in retention. The stability observed under accelerated degradation conditions, in comparison with traditional silanization, was attributed to the polymeric nature of the phenylene layer formed around the silica particles, similar to those formed *via* diazotization on metals.[8,24,69,70]

It is important to point out that the conditions of the degradation test are not typical of LC separations. The degradation test, combining low pH and elevated temperatures, was designed to erode the column life very quickly to provide an indication of the long (or short) lifetime of the stationary phase.[1,64] In many instances, the mobile phase conditions of the test are not typical of HPLC separations; however, it is well known that high-temperature LC can offer several advantages, including faster analysis time, improved efficiency, and organic solvent reduction.[71,72] Elevated temperatures has been beneficial in, for example, proteomic analysis and in pharmaceutical applications.[73,74] Stable columns are required for such applications and clearly, the *p*-PDA-derived particles showed superior stability compared to that prepared *via* conventional silanization.

To illustrate the potential use of the phenylene-like *p*-PDA-derived stationary phase, a peptide standard mixture containing 10 peptides (Agilent 10 PepMix) was separated under acidic conditions using a column packed with 2 μm particles containing the *p*-PDA-derived phase (4 rings per nm$^2$). The resulting chromatogram is shown in Fig. 7. The 10 PepMix is designed for evaluating system suitability and assessing column performance in reversed-phase chromatography, especially in the context of peptide mapping applications. The relatively short column (50 mm length) facilitated separation of the peptide mixture with minimal effort to optimize the separation conditions. The separation of the same sample mixture on a commercially available C18-column (Fig. S4 in SI) can be used as a benchmark to compare the column with the *p*-PDA-derived phase. As anticipated, the longer commercial column provided enhanced resolution than the shorter *p*-PDA-derived column. Although the *p*-PDA-derived column was not expected to perform identically to the commercially available C-18

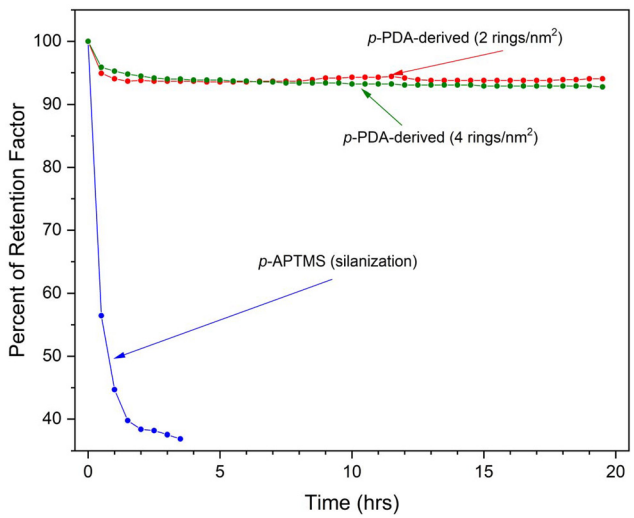


**Fig. 6** Percentage of initial retention factor as a function of time exposed to acidic conditions for three columns packed with Halo® core–shell silica particles with phases prepared by diazotization of *p*-PDA and silanization of *p*-APTMS. Test conditions: 50 : 50 water: acetonitrile with 0.5% TFA, 80 °C, flow rate of 0.2 mL min$^{-1}$. Propylbenzene was used as the retention marker.

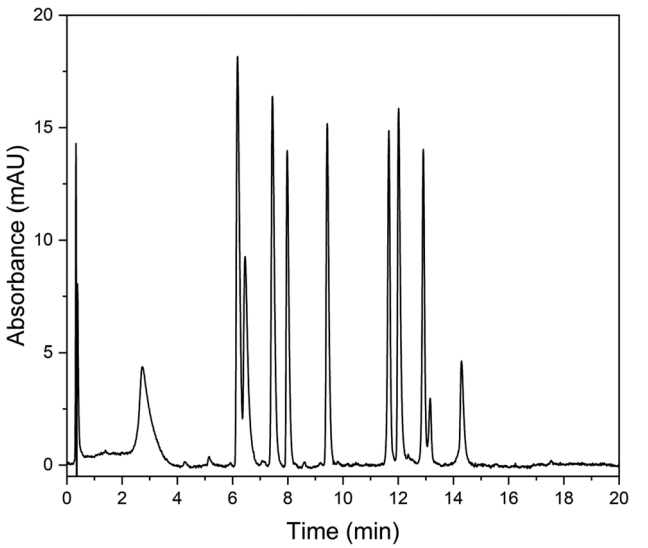


**Fig. 7** Chromatogram illustrating the separation of 10 peptides in a sample mixture. Column: *p*-PDA-derived column, 2.1 mm × 50 mm, 2 μm particles. Separation conditions: gradient 7 AcN (0.08%TFA) : 93 $H_2O$ (0.1% TFA) to 65 : 35 in 25 min at 0.4 mL min$^{-1}$. Injection volume of 2 μL. The standard sample mixture contained: bradykin frag (1–7), bradykin acetate, angiotensin II, neurotensin, angiotensin I, renin, [Ace-F-3,-2 H-1] angiotensinogen (1–14), Ser/Thr protein phosphotase (15–31), [F14] Ser/Thr protein phosphotase (15–31) and Mellitin (0.71 μg μL$^{-1}$ ea.).

Open Access Article. Published on 25 2025. Downloaded on 05.01.2026 23:39:58.
This article is licensed under a Creative Commons Attribution 3.0 Unported Licence.

column, it is noteworthy that the selectivity behavior observed with the *p*-PDA-derived stationary phase differed from the traditional alkyl-based column. Further investigations, which are out beyond the scope of this report, are undoubtedly required to fully understand the use of the *p*-PDA-derived stationary phase for the separation of peptides. Nonetheless, it is evident that the *p*-PDA-derived column showed a significant potential for peptide separation.

## Conclusions

The diazotization of *p*-PDA was used to synthesize a phenylene-like layer on the surface of the core–shell silica particles. The thickness of this silica surface-bound layer was modulated by varying the reaction time and reagents concentration, with successful outcomes achieved at both low (3 °C) and ambient (23 °C) temperatures. XPS data revealed that the *p*-PDA-derived layer contained approximately one nitrogen atom for every three aromatic rings, attributed to the presence of azo and amino groups, equating to approximately one amine group per four to five benzene rings. These findings were consistent with the elemental analysis results. Silica particles with a *p*-PDA-derived layer density of 2–4 rings per $nm^2$ when packed into columns were demonstrated to be suitable for HPLC separation. An accelerated stability test indicated that the *p*-PDA-derived layer was stable under harsh acidic conditions at elevated temperatures (0.5% trifluoroacetic acid, 80 °C), with less than a 5% reduction in retentivity after exposure to 2400 column volumes under such conditions. Preliminary results suggest that the *p*-PDA-derived phase holds promise for peptide separation, an application that is currently under investigation in our laboratory. The retention mechanism for the probe compounds followed that of reversed phase chromatography with methylene selectivity of 1.5 ($k_{amylbenzene}/k_{butylbenzene}$) using the Tanaka[75] test, which is in the range of those typical of C18 columns (*i.e.*, 1.3–1.6).[76] However, further investigations are necessary to explore the selectivity that may have been imparted by the aminated phenyl groups on the stationary phase since the Tanaka test was not designed to capture such. Ongoing work in our laboratory is exploring the use of the linear solvation energy relationship (LSER) model,[77] which we have used previously,[78] to examine the selectivity of the *p*-PDA-derived phase on silica. Overall, we demonstrated that diazotization of *p*-PDA is a viable method for modifying silica particulates for use in HPLC chromatographic columns.

## Author contributions

J. R. Ezzo: conceptualization, methodology, investigation, initial analysis, visualization, writing – original draft; B. L. Salazar: conceptualization, investigation, methodology, validation, formal analysis, visualization, writing – review and editing; R. J. Díaz-Santiago: investigation, validation, visualization, review & editing; L. A. Colón: supervision, conceptualization, methodology, project administrator, funding acquisition, writing – review & editing.

## Conflicts of interest

The authors have no conflicts to declare.

## Data availability

Data supporting the findings reported in this article have been included in the supplementary information (SI). The data include XPS spectra, elemental analysis results and surface coverage under different synthetic conditions, and chromatographic metrics. Supplementary information is available. See DOI: **https://doi.org/10.1039/d5an00869g**.

## Acknowledgements

This work was financially supported by the USA National Science Foundation (CHE 2305066 and CHE 1508105). Any opinions, findings, conclusions or recommendations expressed in this report are strictly those of the authors and do not necessarily reflect the views of the National Science Foundation. We also thank Jason A. Anspach from Phenomenex, Inc. for providing the Kinetex® particles to initiate this project. Additionally, we acknowledge Joseph DeStefano from Advanced Materials Technologies, Inc. (AMT) for the substantially discounted Halo® particles and Stephanie A. Schuster, also from AMT, for the initial column packing of the very early Halo® particles modified *via* diazotization.

## References

1 U. D. Neue, *HPLC Columns: Theory, Technology, and Practice*, Wiley-VCH, New York, 1997.
2 R. E. Majors and M. J. Hopper, *J. Chromatogr. Sci.*, 1974, **12**, 767–778.
3 K. K. Unger, *Packings and Stationary Phases in Chromatographic Techniques*, Marcel Dekker, New York, 1990.
4 M. Delamar, R. Hitmi, J. Pinson and J. M. Saveant, *J. Am. Chem. Soc.*, 1992, **114**, 5883–5884.
5 D. Belanger and J. Pinson, *Chem. Soc. Rev.*, 2011, **40**, 3995–4048.
6 R. L. McCreery, *Chem. Rev.*, 2008, **108**, 2646–2687.
7 S. Mahouche-Chergui, S. Gam-Derouich, C. Mangeney and M. M. Chehimi, *Chem. Soc. Rev.*, 2011, **40**, 4143–4166.
8 *Aryl Diazonium Salts: New Coupling Agents in Polymer and Surface Science*, ed. M. M. Chehimi, Wiley-VCH Verlag GmbH & Co. KGaA, 2012.
9 P. A. Brooksby and A. J. Downard, *Langmuir*, 2004, **20**, 5038–5045.

 This journal is © The Royal Society of Chemistry 2025

Open Access Article. Published on 25 2025. Downloaded on 05.01.2026 23:39:58.
This article is licensed under a Creative Commons Attribution 3.0 Unported Licence.

10 J. Lehr, B. E. Williamson and A. J. Downard, *J. Phys. Chem. C*, 2011, **115**, 6629–6634.
11 A. Mesnage, X. Lefèvre, P. Jégou, G. Deniau and S. Palacin, *Langmuir*, 2012, **28**, 11767–11778.
12 H. Mahjoubi, J. M. Kinsella, M. Murshed and M. Cerruti, *ACS Appl. Mater. Interfaces*, 2014, **6**, 9975–9987.
13 Q. Wang, A. Vasilescu, Q. Wang, Y. Coffinier, M. Li, R. Boukherroub and S. Szunerits, *ACS Appl. Mater. Interfaces*, 2017, **9**, 12823–12831.
14 X. Li, F. Forouzandeh, A. J. Kakanat, F. Feng, D. W. H. Banham, S. Ye, D. Y. Kwok and V. Birss, *ACS Appl. Mater. Interfaces*, 2018, **10**, 2130–2142.
15 J. O. Adongo, T. J. Neubert, G. Sun, S. Janietz, I. Lauermann, K. Rademann and J. Rappich, *ACS Appl. Mater. Interfaces*, 2017, **9**, 24273–24281.
16 A. Mesnage, G. Deniau and S. Palacin, *RSC Adv.*, 2013, **3**, 13901–13906.
17 R. Bangle, R. N. Sampaio, L. Troian-Gautier and G. J. Meyer, *ACS Appl. Mater. Interfaces*, 2018, **10**, 3121–3132.
18 K. Brymora, J. Fouineau, A. Eddarir, F. Chau, N. Yaacoub, J.-M. Grenèche, J. Pinson, S. Ammar and F. Calvayrac, *J. Nanopart. Res.*, 2015, **17**, 438.
19 N. Griffete, F. Herbst, J. Pinson, S. Ammar and C. Mangeney, *J. Am. Chem. Soc.*, 2011, **133**, 1646–1649.
20 J. A. Harnisch, D. B. Gazda, J. W. Anderegg and M. D. Porter, *Anal. Chem.*, 2001, **73**, 3954–3959.
21 S. D. Chambers, M. T. McDermott and C. A. Lucy, *Analyst*, 2009, **134**, 2273–2280.
22 M. F. Wahab, M. E. A. Ibrahim and C. A. Lucy, *Anal. Chem.*, 2013, **85**, 5684–5691.
23 M. F. Wahab, C. A. Pohl and C. A. Lucy, *Analyst*, 2011, **136**, 3113–3120.
24 C. Du, M. Chen, L. Wang and G. Yin, *J. Mater. Chem.*, 2011, **21**, 15692–15697.
25 H. Gong, N. Li and Y. Qian, *Int. J. Electrochem. Sci.*, 2013, **8**, 9811–9817.
26 N. Griffete, J.-F. Dechezelles and F. Scheffold, *Chem. Commun.*, 2012, **48**, 11364–11366.
27 N. Griffete, R. Ahmad, H. Benmehdi, A. Lamouri, P. Decorse and C. Mangeney, *Colloids Surf., A*, 2013, **439**, 145–150.
28 M. Sandomierski, B. Strzemiecka, M. M. Chehimi and A. Voelkel, *Langmuir*, 2016, **32**, 11646–11654.
29 N. Tanaka and D. V. McCalley, *Anal. Chem.*, 2016, **88**, 279–298.
30 S. Fekete, E. Oláh and J. Fekete, *J. Chromatogr. A*, 2012, **1228**, 57–71.
31 G. Guiochon and F. Gritti, *J. Chromatogr. A*, 2011, **1218**, 1915–1938.
32 A. C. Borges-Muñoz, D. P. Miller, E. Zurek and L. A. Colón, *Microchem. J.*, 2019, **147**, 263–268.
33 S. Brunauer, P. H. Emmett and E. Teller, *J. Am. Chem. Soc.*, 1938, **60**, 309–319.
34 E. P. Barrett, L. G. Joyner and P. P. Halenda, *J. Am. Chem. Soc.*, 1951, **73**, 373–380.
35 J. Pinson and F. Podvorica, *Chem. Soc. Rev.*, 2005, **34**, 429–439.
36 D. F. DeTar and S. V. Sagmanli, *J. Am. Chem. Soc.*, 1950, **72**, 965–969.
37 J. B. Lambert, H. F. Shurvell, D. A. Lightner and R. G. Cooks, *Organic Structural Spectroscopy*, Prentice Hall, Upper Saddle River, 1998.
38 N. Chiboub, R. Boukherroub, N. Gabouze, S. Moulay, N. Naar, S. Lamouri and S. Sam, *Opt. Mater.*, 2010, **32**, 748–752.
39 R. Al-Oweini and H. El-Rassy, *J. Mol. Struct.*, 2009, **919**, 140–145.
40 L. Etgar, G. Schuchardt, D. Costenaro, F. Carniato, C. Bisio, S. M. Zakeeruddin, M. K. Nazeeruddin, L. Marchese and M. Graetzel, *J. Mater. Chem. A*, 2013, **1**, 10142–10147.
41 C. A. Capozzi, L. D. Pye and R. A. Condrate, *Mater. Lett.*, 1992, **15**, 130–136.
42 G. D. Chukin and V. I. Malevich, *J. Appl. Spectrosc.*, 1977, **26**, 223–229.
43 T. Menanteau, E. Levillain and T. Breton, *Langmuir*, 2014, **30**, 7913–7918.
44 A. J. Cresswell, S. G. Davies, P. M. Roberts and J. E. Thomson, *Chem. Rev.*, 2015, **115**, 566–611.
45 G. Beamson, D. T. Clark, N. W. Hayes and D. S.-L. Law, *Surf. Sci. Spectra*, 1994, **3**, 357–365.
46 L. Sharma, T. Matsuoka, T. Kimura and H. Matsuda, *Polym. Adv. Technol.*, 2002, **13**, 481–486.
47 E. M. Dief, T. Li, I. Ponce and N. Darwish, *Small*, 2025, **21**, 2412438.
48 A. Kaur, P. Chahal and T. Hogan, *IEEE Electron Device Lett.*, 2016, **37**, 142–145.
49 A. Avila, I. Montero, L. Galán, J. M. Ripalda and R. Levy, *J. Appl. Phys.*, 2001, **89**, 212–216.
50 L. M. Miller and J. Coates, Interpretation of Infrared Spectra, A Practical Approach in *Encyclopedia of Analytical Chemistry*, John Wiley & Sons, Ltd, Online, 2025, pp. 1–24.
51 B. Ashourirad, P. Arab, A. Verlander and H. M. El-Kaderi, *ACS Appl. Mater. Interfaces*, 2016, **8**, 8491–8501.
52 L.-J. Zhu, L.-P. Zhu, P.-B. Zhang, B.-K. Zhu and Y.-Y. Xu, *J. Colloid Interface Sci.*, 2016, **468**, 110–119.
53 Q. Huang, M. Liu, L. Mao, D. Xu, G. Zeng, H. Huang, R. Jiang, F. Deng, X. Zhang and Y. Wei, *J. Colloid Interface Sci.*, 2017, **499**, 170–179.
54 W. Meyer, M. Grunze, R. Lamb, A. Ortega-Vilamil, W. Schrepp and W. Braun, *Surf. Sci.*, 1992, **273**, 205–218.
55 Y. Jian, Y.-J. He, C. Hu, X. Li and P.-N. Liu, *Org. Lett.*, 2024, **26**, 8492–8497.
56 E. M. Borges and M. R. Euerby, *J. Pharm. Biomed. Anal.*, 2013, **77**, 100–115.
57 J. W. Dolan, *LCGC North Am.*, 2017, **35**, 22–28.
58 Z. Wang, H. Ma, K. Smith and S. Wu, *Int. J. Mass Spectrom.*, 2018, **427**, 43–51.
59 F. E. Kuhlmann, A. Apffel, S. M. Fischer, G. Goldberg and P. C. Goodley, *J. Am. Soc. Mass Spectrom.*, 1995, **6**, 1221–1225.

Open Access Article. Published on 25 2025. Downloaded on 05.01.2026 23:39:58.
This article is licensed under a Creative Commons Attribution 3.0 Unported Licence.

60 A. Apffel, S. Fischer, G. Goldberg, P. C. Goodley and F. E. Kuhlmann, *J. Chromatogr. A*, 1995, **712**, 177–190.
61 A. B. Chakraborty and S. J. Berger, *J. Biomol. Tech.*, 2005, **16**, 327–335.
62 T. M. Annesley, *Clin. Chem.*, 2003, **49**, 1041–1044.
63 D. Temesi and B. Law, *LCGC North Am.*, 1999, **17**, 626–630.
64 B. M. Wagner, S. A. Schuster, B. E. Boyes, W. L. Miles, D. R. Nehring and J. J. Kirkland, *LCGC North Am.*, 2015, **33**, 856–865.
65 D. V. McCalley, *J. Chromatogr. A*, 2011, **1218**, 2887–2897.
66 T. Teutenberg, K. Hollebekkers, S. Wiese and A. Boergers, *J. Sep. Sci.*, 2009, **32**, 1262–1274.
67 B. C. Trammell, C. A. Boissel, C. Carignan, D. J. O'Shea, C. J. Hudalla, U. D. Neue and P. C. Iraneta, *J. Chromatogr. A*, 2004, **1060**, 153–163.
68 J. Haun, K. Oeste, T. Teutenberg and T. C. Schmidt, *J. Chromatogr. A*, 2012, **1263**, 99–107.
69 X. T. Le, N. D. Doan, T. Dequivre, P. Viel and S. Palacin, *ACS Appl. Mater. Interfaces*, 2014, **6**, 9085–9092.
70 L. Laurentius, S. R. Stoyanov, S. Gusarov, A. Kovalenko, R. Du, G. P. Lopinski and M. T. McDermott, *ACS Nano*, 2011, **5**, 4219–4227.
71 D. Guillarme and S. Heinisch, *Sep. Purif. Rev.*, 2005, **34**, 181–216.
72 C. V. McNeff, B. Yan, D. R. Stoll and R. A. Henry, *J. Sep. Sci.*, 2007, **30**, 1672–1685.
73 D. Guillarme, R. Russo, S. Rudaz, C. Bicchi and J.-L. Veuthey, *Curr. Pharm. Anal.*, 2007, **3**, 221–229.
74 A. R. Blackler, A. E. Speers and C. C. Wu, *Proteomics*, 2008, **8**, 3956–3964.
75 K. Kimata, K. Iwaguchi, S. Onishi, K. Jinno, R. Eksteen, K. Hosoya, M. Araki and N. Tanaka, *J. Chromatogr. Sci.*, 1989, **27**, 721–728.
76 M. Euerby and P. Petersson, *J. Chromatogr. A*, 2003, **994**, 13–36.
77 X. Subirats and M. Rosés, *J. Chromatogr. A*, 2025, **1762**, 466376.
78 A. C. Borges-Muñoz and L. A. Colón, *J. Sep. Sci.*, 2016, **39**, 3469–3476.


This journal is © The Royal Society of Chemistry 2025